JOURNAL OF CATALYSIS **176,** 439–447 (1998)
ARTICLE NO. CA982084

Reaction Pathway and Stereoselectivity of Olefin Metathesis at High Temperature

B. Bartlett, M. M. Hossain, and W. T. Tysoe[1]

Department of Chemistry and Laboratory for Surface Studies, University of Wisconsin-Milwaukee, Milwaukee, Wisconsin 53201

Received June 11, 1997; revised March 16, 1998; accepted March 16, 1998

The reactions of ethylene and propylene catalyzed by molybdenum model catalysts are examined at high temperature (800–880 K). Hydrocarbon products up to C_6 are present in measurable amounts for both reactions, and products up to C_8 are observed. The product distributions obtained are well described by a Schulz–Flory distribution, where a plot of $\ln(r_n/n)$ versus n yields a straight line, indicating that products are formed by a chain-polymerization mechanism. Analysis of the slopes and intercepts of the Schulz–Flory distributions allows the kinetic parameters for high-temperature metathesis to be estimated. For ethylene, degenerate metathesis is determined to proceed with a reaction order of 1.3 ± 0.2 and an activation energy of 55 ± 7 kcal/mol. The metathesis of propylene is determined to have a reaction order of 1.02 ± 0.05 and an activation energy of 53 ± 3 kcal/mol. Propylene metathesis exhibits stereoselectivity for cis-2-butene formation that is two to three times greater than that predicted thermodynamically. This is suggested to be the result of the geometry necessary for methylcarbene recombination in the context of the proposed mechanism.

INTRODUCTION

Alkene metathesis was first observed in 1931 by Schneider and Frölich when ethylene and butene products were observed after pyrolysis of propylene at 1130 K (1). In 1964, the metathesis of propylene was found to be catalyzed in heterogeneous phase by alumina-supported molybdenum oxide (2). Three years later, homogeneous-phase metathesis catalysis was first observed (3). Since that time, a tremendous amount of work has been done to study the mechanism of metathesis catalysis, and several possible pathways have been proposed. Primary among the mechanisms proposed are the quasi-cyclobutane mechanism (4–12), the metallacyclopropane mechanism (13, 14), and the carbene-metallacycle mechanism (15–29). The carbene-metallacycle mechanism is now the generally accepted mechanism for this reaction, based mostly on results obtained in the homogeneous phase, and the activation energy associated with this mechanism is about 6–9 kcal/mol (30, 31). This carbene mechanism is proposed to be initiated by formation of a carbene active site by olefin reaction with the metal. This metal–carbene may further react with another alkene forming a metallacycle, which can decompose by the reverse of its formation pathway to yield metathesis products. Our work extends these studies to well-characterized model systems (32–34).

A common problem during metathesis catalysis is the loss of product selectivity at higher temperature (>600 K) due to the formation of methane, 1 butene, and higher hydrocarbons (35). It has been found that metallic molybdenum can catalyze propylene metathesis above ~650 K (36, 37). However, the reaction proceeds with an extremely high activation energy (65 ± 5 kcal/mol) and poor selectivity. In addition, higher hydrocarbons are observed in the reaction products (38). Metathesis has also been catalyzed by a MoO_2 model catalyst, where it is found that metathesis products are observed in two regimes (39). In one regime, below ~650 K, formation of ethylene and butene from propylene is found to proceed with a high selectivity (~90%), an absolute rate comparable to that observed on supported catalysts with high molybdenum loading, and an activation energy of 6 ± 2 kcal/mol. It is likely that the accepted carbene-metallacycle mechanism operates under these conditions. However, above 650 K, another mechanism dominates where the activation energy observed for product formation is 60 ± 2 kcal/mol, similar to the value found for metathesis catalyzed by metallic molybdenum, the selectivity is poor, and higher hydrocarbon products are observed. It seems likely that this high-temperature mechanism may be responsible for higher hydrocarbon formation and loss of selectivity in working catalysts at the upper limit of their operating temperature range, as well as carbene active site removal at lower temperature.

Surface science experiments on molybdenum metal and oxygen modified molybdenum have shown that olefinic bond scission and carbene formation is facile below room temperature (32–34). It seems reasonable that, at sufficiently high temperature, metathesis product formation would be the result of direct recombination of carbenes on

[1] Author to whom correspondence should be addressed. E-mail: wtt@csd.uwm.edu.

0021-9517/98 $25.00

the catalyst surface, and that higher hydrocarbon products are formed by polymerization of these surface carbenes. This work examines the viability of this mechanism for the description of the product distributions obtained for the molybdenum-metal catalyzed reactions of ethylene and propylene in this high-temperature regime and is also used to rationalize the observed stereoselectivity of the 2-butene formed from propylene.

EXPERIMENTAL

The apparatus used for these experiments has been described in detail elsewhere (40). Briefly, it consists of a bakeable, stainless-steel ultrahigh vacuum chamber operating at a base pressure of $\sim 1 \times 10^{-10}$ Torr after baking. The chamber is equipped with a quadrupole mass spectrometer for temperature-programmed desorption experiments and a cylindrical-mirror, electron energy analyzer, used for obtaining Auger electron spectra. In addition, an isolateable, high-pressure recirculating batch reactor is incorporated into the ultrahigh vacuum chamber that allows catalytic reactions to be carried out *in situ* at pressures up to one atmosphere while maintaining a pressure of about 1×10^{-9} Torr in the rest of the apparatus. The reaction mixture may be analyzed by diverting small samples to a gas chromatograph equipped with a flame-ionization detector. The output of the detector is connected to a PC through a Keithley picoammeter used as an amplifier and current-voltage converter. This arrangement allows detection of product partial pressures of $<1 \times 10^{-3}$ Torr. Reaction rates are calculated from the product accumulation curves and normalized to the number of exposed atoms on the surface of the foil, taken as equal to the unit cell density on a Mo(100) surface (1×10^{15} cm^{-2}).

Molybdenum foil used is from Aesar and is 99.9999% pure. The foil is cleaned using a standard procedure and is judged free of contamination when no carbon or oxygen signals may be detected with Auger electron spectroscopy. Ethylene and propylene used (Linde, CP grade) is transferred from the cylinder and further purified by bottle-to-bottle distillation. Cleanliness of the reactants is verified by gas chromatography and mass spectroscopy, and the purified reactants are stored in glass until used. Nitrogen (Linde, prepurified grade) gas is used as a ballast and is used as supplied.

RESULTS

Based on the generally accepted mechanism for metathesis, the reaction of ethylene is expected to simply yield ethylene and, thus, produce no products that are measurable without the aid of isotopic labeling. However, in the studied temperature range between 800 and 880 K, measurable accumulations of methane and hydrocarbon products between C_3 and C_6 are observed, and products up to C_8 are detected from the reaction of ethylene catalyzed by metallic molybdenum. It has been shown in ultrahigh vacuum that ethylene can dissociate to form C_1 species (32). It has also been demonstrated that molybdenum is an active CO hydrogenation catalyst where C_3 hydrocarbons are formed by polymerization of C_1 species synthesized from CO and hydrogen (41). It is therefore likely that C_1 species formed from ethylene dissociation can similarly polymerize. If this hypothesis is true, the higher hydrocarbons observed in the products from this reaction should be the result of carbene recombination, then a Schulz–Flory plot of $\ln(r_n/n)$ versus n, where n is the carbon number, and r_n is the yield of product C_n, should yield a straight line. Figure 1 shows the product distribution for the reaction of 450 Torr of ethylene at 870 K catalyzed by molybdenum plotted in this way. This treatment of the data clearly shows a linear relationship, confirming that the observed products are synthesized via polymerization of a C_1 monomer on the catalyst surface. Similar plots are obtained for the product distributions observed under all conditions studied.

Extension of this model to the reaction of propylene catalyzed by molybdenum suggests that metathesis products and higher hydrocarbons observed in the product

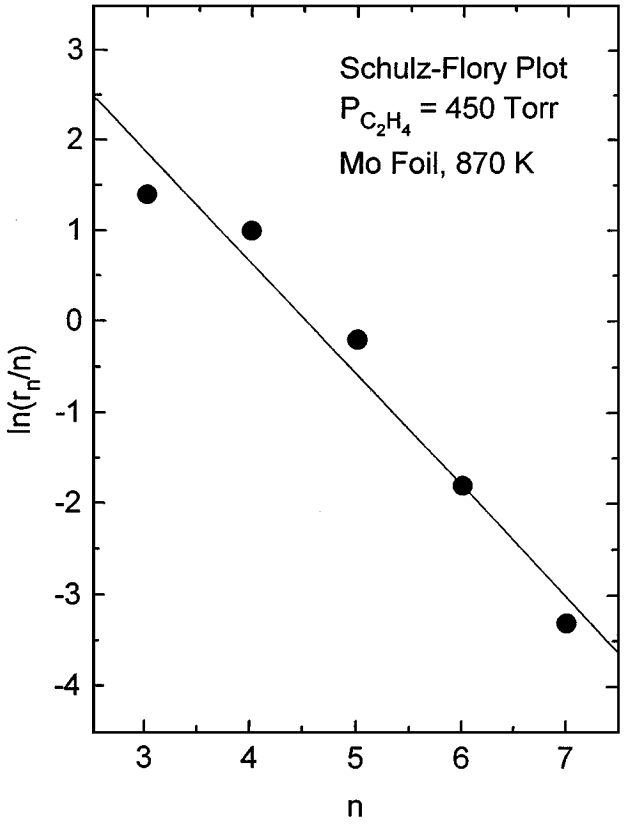

FIG. 1. A typical Schulz–Flory plot for the product distribution from the reaction of ethylene catalyzed by molybdenum at 870 K using 450 Torr of ethylene.

distribution may be formed by copolymerization of carbenes and methylcarbenes. Experiments on propylene adsorbed on Mo(100) and oxygen-covered Mo(100) demonstrate that propylene olefinic bonds also cleave rather easily on these surfaces (32, 42). If it is assumed that equimolar amounts of the C_1 and C_2 monomers formed from the propylene dissociation have similar reactivities and that products may only be formed by combination with a monomer unit, then a theoretical product distribution may be calculated based on a consideration of the various chain combinations which may form each carbon number C_n. Figure 2 displays the results of this calculation for the reaction of 200 Torr of propylene catalyzed by molybdenum at 865 K compared to the experimentally observed product distribution in histogram form. The C_3 product yield is not plotted since any propylene formed metathetically cannot be distinguished from the reactant. The calculated product distribution is normalized to the amount of C_4 products observed and agrees well with that found experimentally. In addition, the theory predicts the reformation rate of propylene and the formation rate of products higher than C_6, which could not be measured since their accumulations were below the detection limit of our equipment. The expected formation rates for some of these products are shown in the calculated distribution.

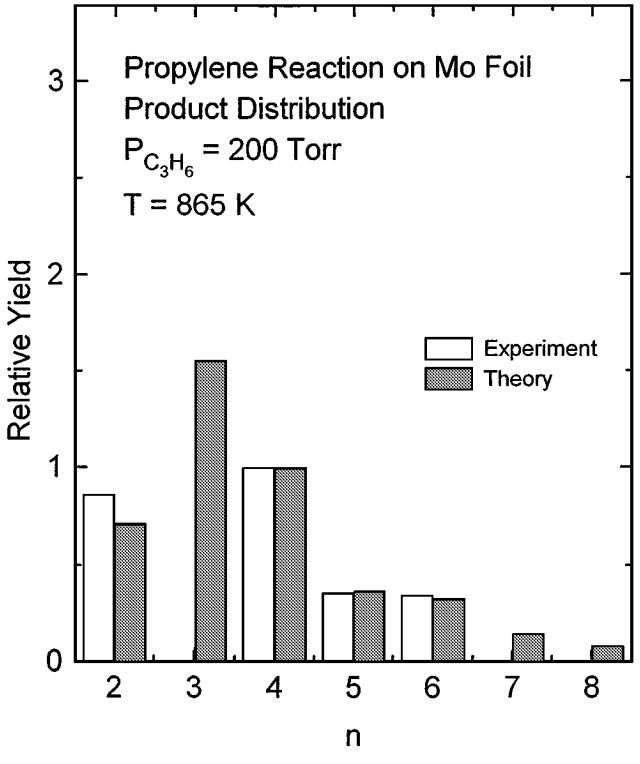

FIG. 2. Histogram comparing the experimental product distribution (■) with that predicted theoretically (□), assuming that higher hydrocarbons for by copolymerization of C_1 and C_2 monomers for the reaction of 200 Torr of propylene at 865 K.

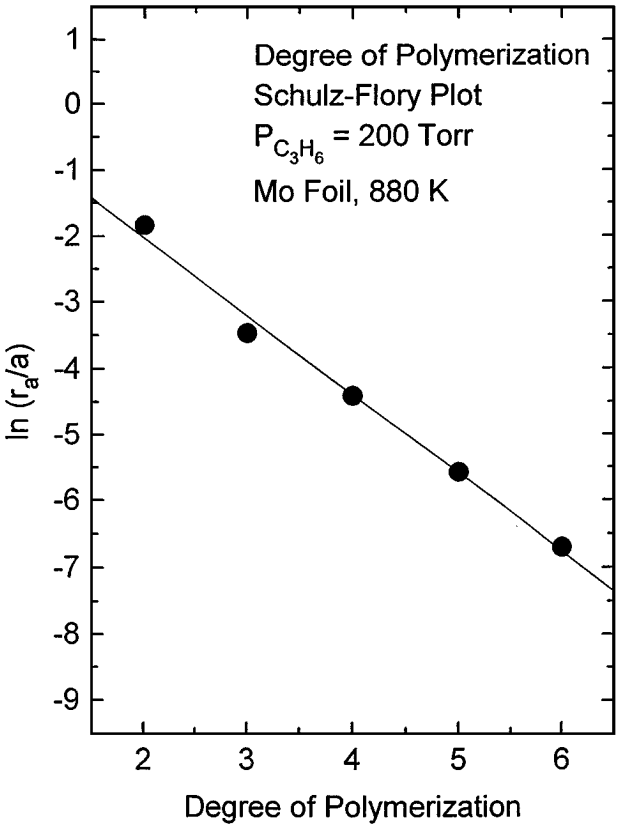

FIG. 3. Schulz–Flory plot for the degree of polymerization product distribution from the reaction of propylene, which plots $\ln(r_a/a)$ versus a, where a is the degree of polymerization.

Since the distribution function calculates the relative formation rates of each possible carbon chain, the function may be used to dissect the experimentally observed product distributions and reassemble them to obtain a product distribution in terms of degree of polymerization. If the assumptions are made that each of the two monomers (C_1 and C_2) have similar reactivities, and that products are formed by chain copolymerization, then a Schulz–Flory plot of the degree-of-polymerization distribution should yield a straight line. Figure 3 shows a plot of $\ln(r_a/a)$ versus a, where a is the degree-of-polymerization and r_a is the yield of all chains with degree a, for the reaction of 200 Torr of propylene catalyzed by molybdenum metal at 880 K. This plot is indeed linear, confirming that the products of this reaction are formed by recombination of C_1 and C_2 monomers with similar reactivities on the molybdenum surface.

It is demonstrated below that the slopes and intercepts of the Schulz–Flory distributions are functions of fundamental rate constants and may, therefore, be expected to exhibit Arrhenius behavior. Figures 4 and 5 show Arrhenius plots of the Schulz–Flory distribution intercepts for molybdenum-catalyzed ethylene and propylene reactions, respectively. Analysis of these data shows that the activation energy for the intercepts obtained from ethylene product

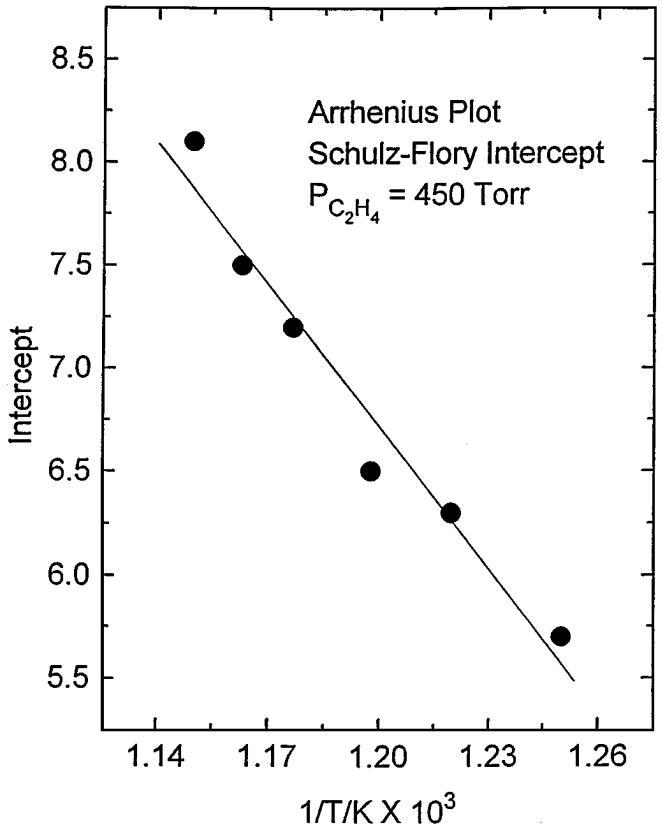

FIG. 4. The intercept of the Schulz–Flory plot for ethylene metathesis catalyzed at high temperature by metallic molybdenum for various temperatures plotted in Arrhenius form.

distributions is 46 ± 4 kcal/mol and the activation energy for the intercepts obtained from degree-of-polymerization distributions of propylene is 42 ± 1 kcal/mol. Similar plots are shown for the slopes of the Schulz–Flory distributions in Figs. 6 and 7, and the activation energies obtained from analysis of these data are 4.6 ± 0.4 kcal/mol for ethylene and 5.4 ± 0.6 kcal/mol for propylene. Further inspection of the functional form of the Schulz–Flory intercept (see below) reveals that this term is expected to contain pressure-dependence information due to its dependence on monomer coverage. Plots of the Schulz–Flory intercept versus ln (reactant pressure) should therefore yield the reaction order for product formation, and these data are displayed in Figs. 8 and 9. The slopes of these plots are the reaction orders, and they are found to be 1.3 ± 0.2 for ethylene and 1.02 ± 0.05 for propylene. Both of these reaction orders agree well with values found previously for high-temperature metathesis catalyzed by molybdenum model catalysts.

Another aspect of the high-temperature reaction of propylene catalyzed by molybdenum and MoO_2 model catalysts is an observed reaction stereoselectivity manifest by differences in activation energy for the formation of the cis and trans isomers of 2-butene. Figure 10 shows the temperature dependence of cis- (●) and trans-2-butene (■) formation for reaction catalyzed by an MoO_2 model catalyst plotted in Arrhenius fashion. Here the rate is calculated as a turnover frequency (reactions/site/s) as described in the Experimental section. These data show that the difference in activation energies observed for the two isomers is 12 ± 3 kcal/mol. This difference in activation energies between the butene isomers results in a stereoselective preference for cis-2-butene versus trans-2-butene, compared to the thermodynamically predicted ratio. Figure 11 shows the cis–trans product ratios for butenes formed from reaction of propylene catalyzed by a MoO_2 model catalyst compared to the thermodynamically predicted value plotted as ratio (reaction)/ratio(thermodynamic) versus temperature. The data shown in this figure indicate that the observed cis/trans ratio for butene products is two to three times higher than is thermodynamically anticipated.

DISCUSSION

The formation of higher hydrocarbons from the reaction of ethylene with a product distribution that is well described

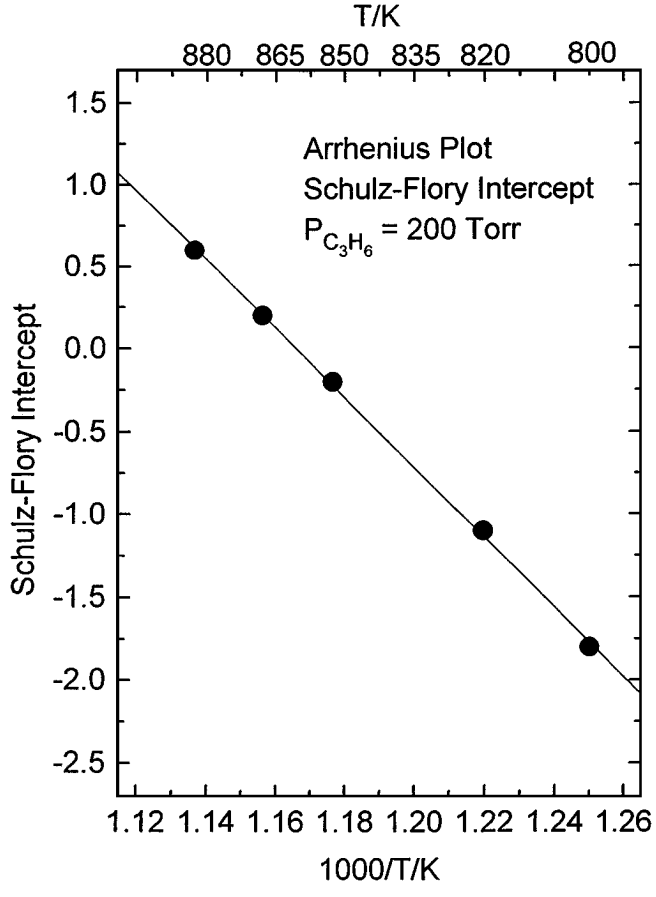

FIG. 5. The intercept of the Schulz–Flory plot for propylene metathesis catalyzed at high temperature by metallic molybdenum for various temperatures plotted in Arrhenius form.

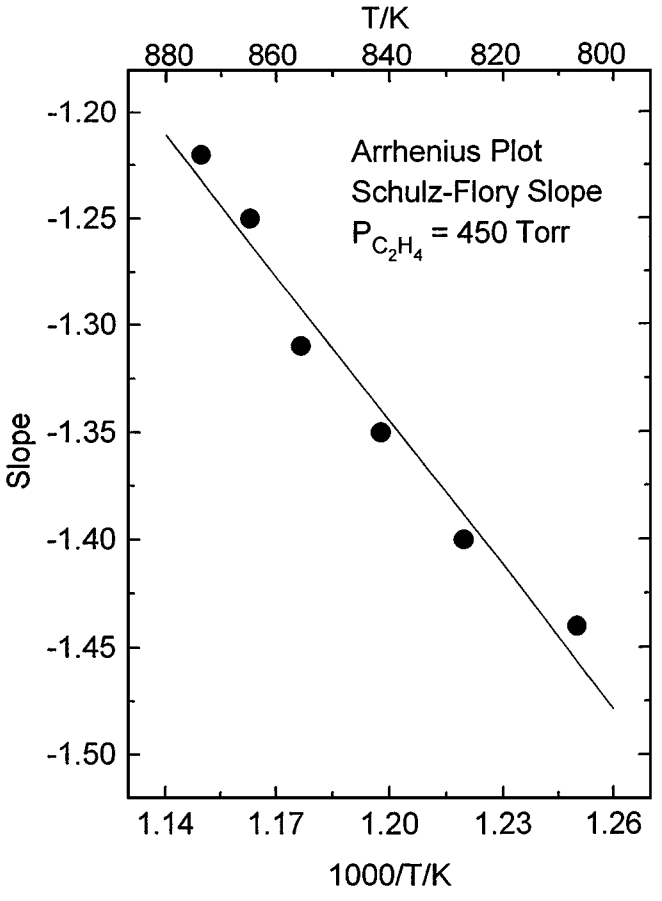

FIG. 6. The slope of the Schulz–Flory plot for ethylene metathesis catalyzed at high temperature by metallic molybdenum for various temperatures plotted in Arrhenius form.

by a Schulz–Flory distribution (Fig. 1) is compelling evidence that these products are the result of oligimerization of C_1 monomers on the catalyst surface. For the reaction of ethylene, it is proposed that initiation of this reaction is by scission of the alkene bond to form surface C_1 species, which may then further react to form surface C_n species (propagation) or gas phase C_n products (termination). This reaction scheme is analogous to the mechanism accepted for Fischer–Tropsch synthesis (43–46).

If the equilibrium coverage of hydrocarbon C_n on the catalyst surface is expressed as θ_n and it is assumed that reaction proceeds by a chain mechanism (where propagation and termination may only occur through reaction with a surface monomer), then the rate of change of each surface species C_n may be expressed as

$$\frac{d\theta_n}{dt} = k_p\theta_1\theta_{n-1} - k_t\theta_1\theta_n - k_p\theta_n\theta_1, \qquad [1]$$

where k_p is the rate constant for chain propagation and k_t is the rate constant for chain termination. Assuming steady-state conditions ($d\theta_n/dt = 0$), this expression yields a recursion relation between θ_n and θ_1,

$$\theta_n = \left(\frac{k_p}{k_t + k_p}\right)^{n-1}\theta_1, \qquad [2]$$

for the relative coverage, θ_n, of each hydrocarbon, C_n. The appearance rate of each C_n product in the gas phase may then be expressed as

$$r_n = k_t\theta_1\theta_{n-1}. \qquad [3]$$

Substitution of Eq. [2] into Eq. [3] yields the Schulz–Flory distribution for each reaction product as

$$\ln\left(\frac{r_n}{n}\right) = n\ln\left(\frac{k_p}{k_t + k_p}\right) + \ln\left(\frac{k_t\theta_1^2}{(k_p/(k_t + k_p))^2}\right). \qquad [4]$$

Therefore, for a plot of $\ln(r_n/n)$ versus n, the slope is given by

$$S = \ln\left(\frac{k_p}{k_t + k_p}\right) \qquad [5]$$

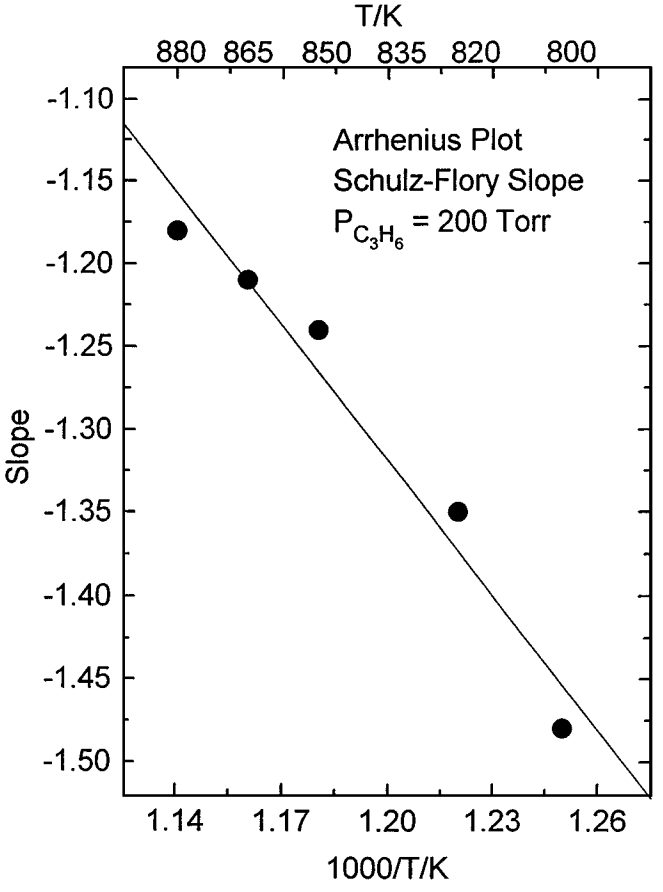

FIG. 7. The slope of the Schulz–Flory plot for propylene catalyzed at high temperature by metallic molybdenum for various temperatures plotted in Arrhenius form.

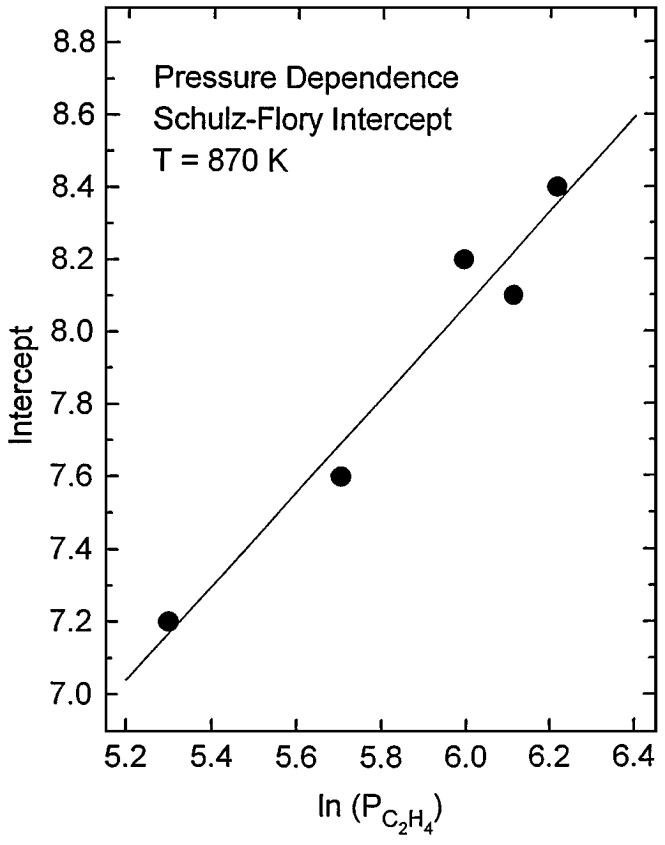

FIG. 8. The intercept of the Schulz–Flory plot for ethylene metathesis catalyzed at high temperature (870 K) by metallic molybdenum plotted versus ln (ethylene pressure).

and the intercept is

$$I = \ln\left(\frac{k_t\theta_1^2}{(k_p/(k_t + k_p))^2}\right). \quad [6]$$

Because these quantities are expressed in terms of logarithms of rate constants, they may be plotted directly against ln(P) and 1/T to yield pressure and temperature dependencies, respectively.

This analysis may be extended to describe the product distribution formed during the reaction of propylene catalyzed by molybdenum model catalysts, assuming that this reaction proceeds via a similar pathway. Unlike ethylene, however, propylene is expected to adsorb on the surface and undergo olefinic bond cleavage to yield equimolar C_1 and C_2 carbenes. For this reason, the reaction should then be described by a chain copolymerization mechanism, where the monomer units are carbenes and methylcarbenes.

Unfortunately, an analytical expression describing the product distribution like that developed above the ethylene cannot be reached directly in the case of propylene, due to the presence of two different monomer units. However, if a chain mechanism is assumed, where termination and propagation proceed only by reaction with a monomer unit, then a relative product distribution may be estimated, based on the relative reactivities of each monomer and their termination probabilities.

In binary copolymerization, if there is an equal reaction probability for the two monomers, then the chance of each monomer existing in a particular place in the chain sequence is 0.5. It follows from this that the probability of a chain consisting of a particular monomer sequence existing is $(0.5)^a$, where a is the degree of polymerization (47). Since, in the case of chain copolymerization, propagation and termination occur only by the addition of a monomer to the end of the chain, this means that, whenever a monomer unit adds to a chain, it has a chance to desorb from the surface to yield product (α) or a chance to propagate to become a longer surface oligomer ($1-\alpha$). It follows from this that for a product of degree of polymerization (a) to form, the particular chain sequence must exist, so that the chain must have propagated ($a-2$) times, and then terminated. The relative proportion of each chain formed as a product is then

$$\frac{r_a}{r_{tot}} = (0.5)^a(1-\alpha)^{a-2}\alpha. \quad [7]$$

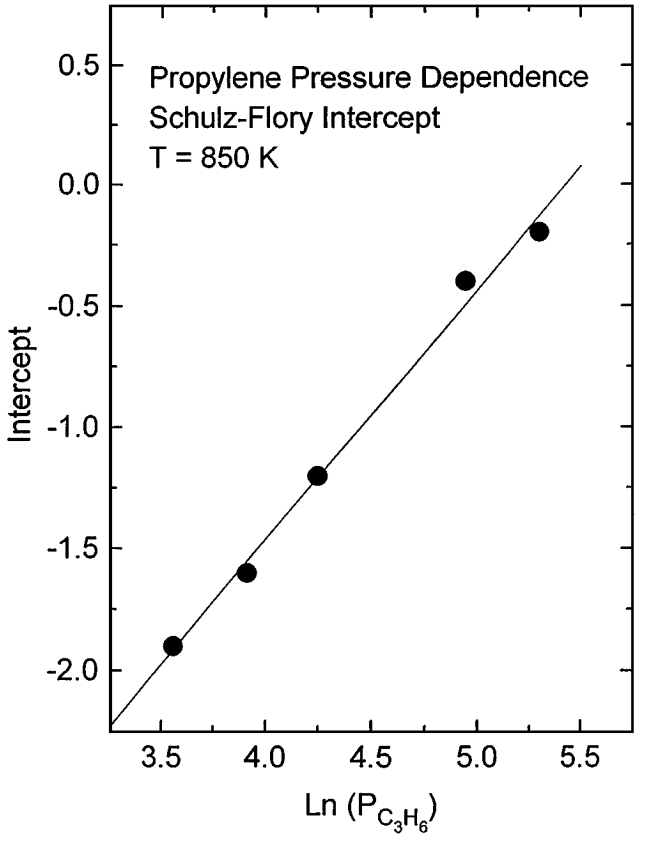

FIG. 9. The intercept of the Schulz–Flory plot for propylene metathesis catalyzed at high temperature (850 K) by metallic molybdenum plotted versus ln (propylene pressure).

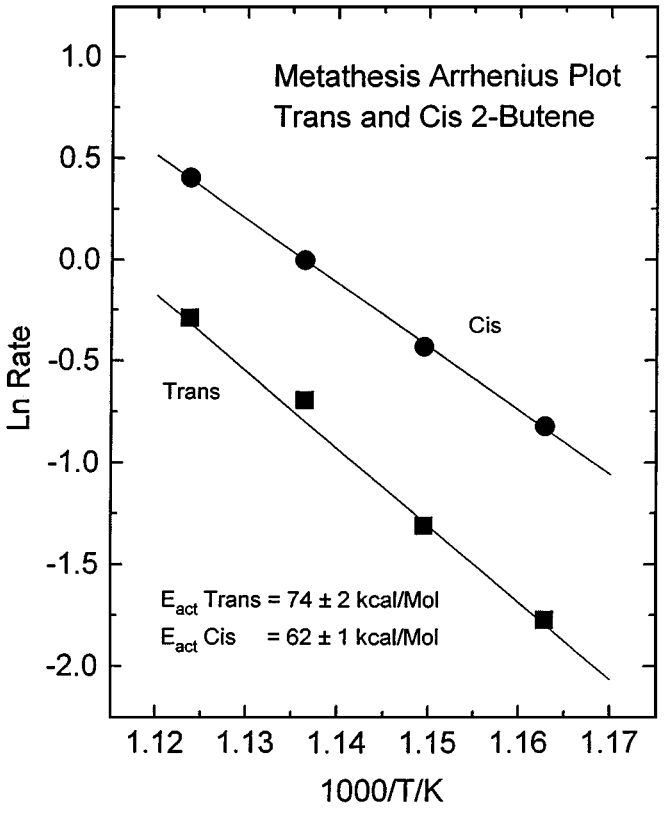

FIG. 10. Arrhenius plots for the formation of cis- (●) and trans-2-butenes (■) from the reaction of 450 Torr of propylene catalyzed by molybdenum dioxide. Rates are measured as turnover frequencies (see Experimental section).

To determine the relative amount of product of carbon number C_n that is formed during reaction, each possible chain that can make that product must be summed. If n is even, then the possible chains formed would range from the degree of polymerization, a, equal to n/2 for chains formed by all C_2 monomers, and n for chains formed by all C_1 monomers. For n odd, this range would be from $(n+1)/2$ for chains formed from all C_2 monomers, except one C_1 unit, to n for chains formed from all C_1 units. Finally, the number of ways each chain of degree a may be formed and terminated is calculated. At this point, we have no simple analytical method of calculating this quantity for all cases, so this number must be calculated manually.

The result of this calculation yields two similar equations, for n even,

$$\frac{r_n}{r_{tot}} = \sum_{n/2}^{n} Q_a (0.5)^a (\alpha - 1)^{a-2} \alpha, \qquad [8]$$

and for n odd,

$$\frac{r_n}{r_{tot}} = \sum_{(n+1)/2}^{n} Q_a (0.5)^a (\alpha - 1)^{a-2} \alpha, \qquad [9]$$

where, in both equations, n is the carbon number, a is the degree of polymerization, Q_a is the number of ways that the chain may be formed, and α is the termination probability. These are the functions used in determining the fit for the product distribution shown in Fig. 2. It should be emphasized here that the values of Q_a are constant, and that α is the only parameter varied to fit each set of experimental data.

Once the value of α is determined by fitting the experimental data, this distribution function allows the product distribution to be expressed in terms of product appearance, based on the degree of polymerization rather than the carbon number. Because of the assumption of equal monomer reactivity, this degree of polymerization distribution is directly comparable to the product distribution obtained from the reaction of ethylene, and thus the product accumulation data from propylene expressed in terms of the degree of polymerization should form a Schulz–Flory distribution. This is confirmed by the data shown in Fig. 3.

In general, the rate of metathesis product formation, which is the result of direct monomer recombination and elimination, may be expressed as

$$r_m = k_t \theta_1^2 \qquad [10]$$

for both ethylene and propylene metathesis, where in this case θ_1 is the total monomer coverage.

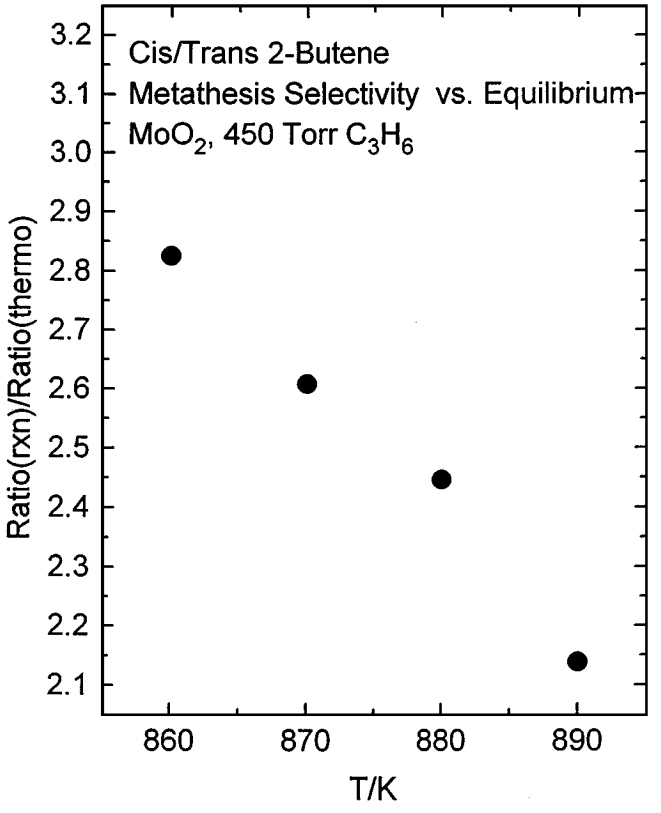

FIG. 11. The cis- to trans-2-butene ratio for propylene metathesis products compared with the thermodynamic ratio of these products using 450 Torr of propylene catalyzed by a MoO_2 model catalyst.

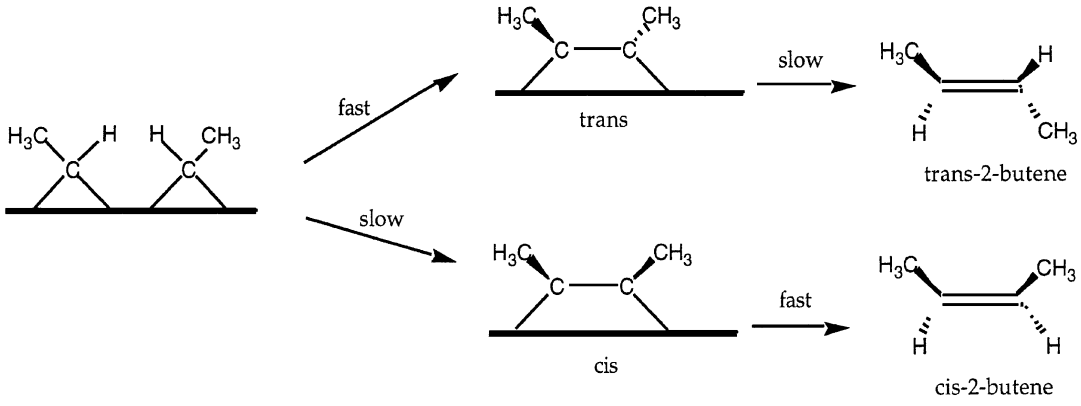

SCHEME 1.

Along with Eqs. [5] and [6], this expression allows the activation energy for metathesis product formation to be estimated, based on the activation energies found from the Schulz–Flory slopes and intercepts (Figs. 4–7). The activation energy contributions for the intercept may be expressed by taking the logarithms of Eq. [6] as

$$E_{act}(I) = E_{act}\left(k_t\theta_1^2\right) - 2E_{act}(k_p/(k_t + k_p)). \qquad [11]$$

Thus, the activation energy for metathesis ($E_{act}(k_t\theta_1^2)$) may be estimated as the intercept activation energy plus twice the slope activation energy ($E_{act}(k_p/(k_t + k_p))$, Eq. [5]). These values are determined to be 55 ± 7 kcal/mol for ethylene metathesis and 53 ± 3 kcal/mol for propylene metathesis, and they are comparable to values previously measured for propylene metathesis product formation under similar conditions.

This recombination pathway for high-temperature metathesis can also be used to rationalize the observed stereoselectivity for cis-2-butene versus trans-2-butene. Figure 11 shows that the preference for the cis isomer is two to three times greater than the thermodynamically predicted ratio for reaction of propylene catalyzed by MoO_2, and a difference of 12 ± 3 kcal/mol in activation energies is found. For the reaction of propylene catalyzed by molybdenum metal, similar stereoselectivity values of about 2 are found. MoO_2 is catalytically more active for high-temperature metathesis that metallic molybdenum, which allows these reaction rate differences to be more accurately measured at lower reaction temperatures than on metallic molybdenum. The recombination mechanism proposed above predicts that butenes are predominantly formed by recombination of surface methylcarbenes. It is assumed that the approach of the methylcarbenes to each other is such that the carbene planes are parallel. This geometry will facilitate overlap between the carbene π orbitals and the formation of the σ and π bonds between the α carbons. In this case, steric hindrance between the methyl groups of the approaching methyl carbenes will favor the formation of a trans-intermediate in this initial step as indicated in Scheme 1. In general, carbene recombination in organometallic compounds leads to the formation of trans products as predicted from this step (48–53). This will lead to the formation of a surface bonded 2-butene species where the carbons are depicted as being sp^3 hybridized. This has been shown to be the case of ethylene adsorbed on metallic molybdenum (54) and so it is likely also to be true for butenes.

The next step is the reductive elimination of this di-σ-bonded metallacyclic intermediate to form 2-butene. This step involves the hybridization of the carbons changing from sp^3 to sp^2 and the molecule becoming planar. When the intermediate is bonded to an isolated metal center, there is no steric hindrance involved with this step. In contrast, when it is adsorbed on a planar substrate, the methyl groups will prevent this molecule rehybdridzing in the case of the trans intermediate. In the case of the cis intermediate, the molecule can rotate slightly about the C(2)-C(3) bond to minimize steric interference between the methyl groups and the surface thereby facilitating product formation as depicted in Scheme 1.

CONCLUSIONS

The reactions of ethylene and propylene at high temperature produce higher hydrocarbons with chain lengths up to C_8. The experimental product distributions are well described by a Schulz–Flory distribution, indicating that products are formed by a chain-polymerization mechanism. The reaction orders determined from analysis of the Schulz–Flory plots indicate that the metathesis reactions are 1.3 ± 0.2 order in ethylene and 1.02 ± 0.05 order in propylene (Figs. 8, 9). The activation energy for degenerate metathesis of ethylene is determined to be 55 ± 7 kcal/mol from the Schulz–Flory plots, and the activation energy for metathesis product formation from the reaction of propylene is found to be 53 ± 3 kcal/mol in the same manner. Both of these values are consistent with values previously

observed for propylene metathesis under similar conditions. Stereoselectivity for cis-2-butene formation is determined to be two to three times greater than thermodynamically anticipated (Figs. 10, 11), and this is analyzed in terms of the carbene recombination model outlined above.

ACKNOWLEDGMENT

We gratefully acknowledge the support of this work by the U.S. Department of Energy, Division of Chemical Sciences, Office of Basic Energy Research, under Grant DE-FG02-92ER14289.

REFERENCES

1. Schneider, V., and Frölich, P. K., *Ind. Eng. Chem.* **23**, 1045 (1931).
2. Banks, R. L., and Bailey, G. C., *Ind. Eng. Chem., Prod. Res. Dev.* **3**, 170 (1964).
3. Calderon, N., Chen, H. Y., and Scott, K. W., *Tetrahedron Lett.* **8**, 3327 (1967).
4. Hughes, W. B., *J. Am. Chem. Soc.* **92**, 532 (1969).
5. Bradshaw, C. P. C., Howman, E. J., and Turner, L., *J. Catal.* **7**, 269 (1967).
6. Adams, C. T., and Brandenberger, S. G., *J. Catal.* **13**, 360 (1969).
7. Crain, D. L., *J. Catal.* **13**, 110 (1969).
8. Mol, J. C., Moulijn, J. A., and Boulhouwer, C., *J. Catal.* **11**, 87 (1969).
9. Woody, F. L., Lewis, M. J., and Willis, G. B., *J. Catal.* **14**, 389 (1969).
10. Clark, A., and Cook, C., *J. Catal.* **15**, 420 (1969).
11. Calderon, N., Ofstead, E. A., Ward, J. P., Judy, W. A., and Scott, K. W., *J. Am. Chem. Soc.* **90**, 4133 (1969).
12. Mango, F. D., and Schnachtschneider, J. H., *J. Am. Chem. Soc.* **89**, 2484 (1967).
13. Grubbs, R. H., and Brunk, T. K., *J. Am. Chem. Soc.* **94**, 2538 (1972).
14. Biefeld, G. C., Eick, H. A., and Grubbs, R. H., *Inorg. Chem.* **12**, 2166 (1973).
15. Hérisson, J. L., and Chauvin, Y., *Makromol. Chem.* **141**, 161 (1970).
16. Casey, C. P., and Burkhardt, J., *J. Am. Chem. Soc.* **96**, 7808 (1974).
17. Schrock, R. R., *J. Am. Chem. Soc.* **96**, 6976 (1974).
18. Schrock, R. R., *J. Am. Chem. Soc.* **98**, 5399 (1976).
19. Dolgoplosk, B. A., *Dokl. Chem.* **216**, 380 (1974).
20. Grubbs, R. H., Burk, P. L., and Carr, D. D., *J. Am. Chem. Soc.* **97**, 3265 (1975).
21. Grubbs, R. H., Carr, D. D., Hoppin, C., and Burk, P. C., *J. Am. Chem. Soc.* **98**, 3478 (1976).
22. Katz, T. J., and Rothschild, J., *J. Am. Chem. Soc.* **98**, 2519 (1976).
23. Katz, T. J., and Hersch, W. H., *Tetrahedron Lett.*, 585 (1977).
24. Casey, C. P., Hunstra, H. E., and Searnan, M. C., *J. Am. Chem. Soc.* **98**, 608 (1976).
25. Howard, T. R., Lee, J. B., and Grubbs, R. H., *J. Am. Chem. Soc.* **102**, 6878 (1980).
26. Grubbs, R. H., and Brunck, T. K., *J. Am. Chem. Soc.* **94**, 25 (1972).
27. Kazuta, M., and Tanaka, K., *Catal. Lett.* **1**, 7 (1988).
28. Vikulov, K. A., Elev, I. V., Shelimov, B. N., and Kazansky, V. B., *Catal. Lett.* **2**, 121 (1989).
29. Wang, L. P., Millman, W. S., and Tysoe, W. T., *Catal. Lett.* **1**, 159 (1988).
30. Davie, E. S., Whan, D. A., and Kemball, C., *J. Catal.* **24**, 272 (1972).
31. Moffat, A. J., and Clark, A., *J. Catal.* **17**, 264 (1970).
32. Wu, G., Bartlett, B., and Tysoe, W. T., *Surf. Sci.* **383**, 57 (1997).
33. Wu, G., and Tysoe, W. T., *Surf. Sci.* **391**, 134 (1997).
34. Wu, Gefei., and Tysoe, W. T., *Surf. Sci.* **397**, 197 (1998).
35. Dragutan, V., Balaban, A. T., and Dimonie, M., "Olefin Metathesis and Ring-Opening Polymerization of Cyclo-Olefins," Wiley, New York, 1985.
36. Wang, L. P., Soto, C., and Tysoe, W. T., *J. Catal.* **128**, 320 (1993).
37. Bartlett, B., Soto, C., Wu, R., and Tysoe, W. T., *Catal. Lett.* **21**, 1 (1993).
38. Bartlett, B., Schneerson, V. L., and Tysoe, W. T., *Catal. Lett.* **32**, 1 (1995).
39. Bartlett, B. F., Molero, H., and Tysoe, W. T., *J. Catal.* **167**, 470 (1997).
40. Wang, L. P., and Tysoe, W. T., *Surf. Sci.* **230**, 74 (1990).
41. Logan, M., Gellman, A. J., and Somorjai, G. A., *J. Catal.* **63**, 226 (1980).
42. Wang, L. P., and Tysoe, W. T., *Surf. Sci.* **245**, 41 (1991).
43. Goodman, D. W., Kelley, R. D., Madey, T. E., and Yates, J. T., Jr., *J. Catal.* **63**, 226 (1980).
44. Young, C. B., and Whiteside, G. N., *J. Am. Chem. Soc.* **100**, 5808 (1978).
45. Biloen, P., Helle, J. N., and Sachtler, W. M. H., *J. Catal.* **58**, 95 (1979).
46. Brady, R. C., and Pettit, R. J., *J. Am. Chem. Soc.* **103**, 1287 (1981).
47. Odian, G., "Principles of Polymerization," Wiley, New York, 1991.
48. Jolly, P. W., and Pettit, R. J., *J. Am. Chem. Soc.* **88**, 5044 (1955).
49. Casey, C. P., and Polichnowski, S. W., *J. Am. Chem. Soc.* **99**, 6097 (1977).
50. Casey, C. P., Polichnowski, S. W., Shusterman, A. J., and Jones, R. C., *J. Am. Chem. Soc.* **101**, 7872 (1979).
51. Fischer, H., Zeuner, S., and Ackermann, K. J., *J. Chem. Soc., Chem. Commun.*, 684 (1984).
52. Brookhart, M., and Nelson, G. O., *J. Am. Chem. Soc.* **99**, 6099 (1977).
53. Brookhart, M., Humphrey, M. B., Kratzer, H. J., and Nelson, G. O., *J. Am. Chem. Soc.* **102**, 7802 (1977).
54. Wang, L. P., and Tysoe, W. T., *Surf. Sci.* **236**, 325 (1990).